Intra-Individual Differences Between Technetium-99m-HMPAO and Technetium-99m-ECD in the Normal Medial Temporal Lobe

Naohiko Oku, Masayasu Matsumoto, Kazuo Hashikawa, Hiroshi Moriwaki, Mariko Ishida, Yujiro Seike, Haruhiko Terakawa, Yoshiyuki Watanabe, Toshiisa Uehara and Tsunehiko Nishimura

Division of Nuclear Medicine, First Department of Medicine and Departments of Neurology and Tracer Kinetics, Osaka University Medical School, Osaka, Japan

Regional distributions of ^{99m}Tc-hexamethyl propyleneamine oxime (^{99m}Tc-HMPAO) and ^{99m}Tc-ethyl cysteinate dimer (^{99m}Tc-ECD) were compared in the normal brain. **Methods:** Six paid, healthy volunteers (mean age 26 yr) had high-resolution neuroperfusion SPECT using both ^{99m}Tc-HMPAO and ^{99m}Tc-ECD on separate days. **Results:** Regional distribution of the two tracers differed. Technetium-99m-HMPAO accumulated more in the thalamus, frontal lobe, temporal lobe and cerebellum than ^{99m}Tc-ECD, which accumulated more in the occipital and parietal lobes. There was a considerable difference in the accumulations of the two tracers in the medial temporal lobe. The percent accumulations of ^{99m}Tc-HMPAO and ^{99m}Tc-ECD in the medial temporal lobe compared with the mean global cerebral cortical accumulation were 93.9% ± 2.4% and 83.1% ± 4.1% (mean ± s.d.), respectively. **Conclusion:** The results suggest that ^{99m}Tc-HMPAO and ^{99m}Tc-ECD require specific and separate criteria for diagnosing temporal lobe pathologies, such as dementia and temporal lobe epilepsy.

Key Words: technetium-99m-HMPAO; technetium-99m-ECD; SPECT; hippocampus

J Nucl Med 1997; 38:1109–1111

The introduction of ^{99m}Tc-labeled neuroperfusion tracers has enabled high-resolution SPECT imaging of the brain. Currently, ^{99m}Tc-hexamethyl propyleneamine oxime (^{99m}Tc-HMPAO) and ^{99m}Tc-ethyl cysteinate dimer (^{99m}Tc-ECD) are commercially available for routine SPECT examinations of central nervous system disorders. These tracers have varying characteristics, and interest has focused on their differential cortical distributions under pathological conditions (*1*). Differences between the regional distributions of these two tracers in the normal brain have not been thoroughly investigated. We compared the distributions of two ^{99m}Tc-labeled neuroperfusion tracers in the normal human brain.

MATERIALS AND METHODS

Subjects

The participants were six paid, healthy volunteers (three men and three women) whose mean age was 26.0 ± 7.9 yr old. None of them was taking medication or had experienced central nervous system disorders of any type. A trained neurologist certified them as free of neurological deficits or memory impairment. The participants were fully informed of the purpose and details of the study, and written informed consent was given by each. One volunteer agreed to participate in an additional PET investigation. This study was performed according to the standard ethical guidelines of Osaka University.

Received Jun. 10, 1996; revision accepted Nov. 23, 1996.

For correspondence or reprints contact: Naohiko Oku, MD, First Department of Medicine, Osaka University Medical School, Yamada-oka 2-2, Suita 565, Osaka, Japan.

Protocol

The SPECT apparatus was a high-performance, four-headed gamma camera system (*2*) equipped with low-energy, high-resolution, parallel-hole collimator (GAMMA VIEW SPECT 2000H, Hitachi Medical Co., Tokyo, Japan). The inplane and axial resolution after reconstruction was 10.0 mm in FWHM. The participants had paired isolated SPECT scans, one for ^{99m}Tc-HMPAO and the other for ^{99m}Tc-ECD. The participants rested supine on the scanning bed with their eyes closed. The room was dimly lit and ambient machine noise was minimized. A butterfly needle was inserted into the antecubital vein and 740 MBq of either ^{99m}Tc-HMPAO or ^{99m}Tc-ECD were administered. Ten minutes later, SPECT acquisition started with a 20-sec per step, 64-step per camera, 360° and 64-pixel (4 × 4 mm per pixel) format. This means that each camera acquired 64 projections of data in a single 360° revolution, and the final dataset consisted of 64 projections of data that were the sum of the data from four cameras. The total acquisition time was approximately 22 min. Three to seven days later, the tested individuals had another tracer session. The head position of each participant was reproduced very carefully by using a machine indwelling positioning crossed light beam. The order of ^{99m}Tc-HMPAO and ^{99m}Tc-ECD sessions was reversed in alternate participants.

One volunteer had additional regional cerebral blood flow (rCBF) measurement by PET (HEADTOME V, Shimadzu Co., Kyoto, Japan). Regional CBF was measured using a $H_2{}^{15}O$ bolus injection and autoradiography (*3*).

Image Analysis

The raw projection SPECT data were transferred to a nuclear medicine-oriented computer (HARP 2, Hitachi Medical Co., Tokyo, Japan). The projection data were prefiltered with a Butterwoth filter (cutoff 0.2 cycles/pixel, order 4) and reconstructed into two series of transaxial images of 8 and 4 mm thick, using Ramachandran's backprojection algorithm. Chang's attenuation correction was applied to the reconstructed images with an attenuation coefficient of 0.08 cm^{-1}. Finally, the 4-mm thick transaxial images were sliced into 4-mm thick hippocampal plane (HP) images (Fig. 1). HP imaging is described in detail elsewhere (*4*). On the 8-mm thick transaxial images, arbitrarily shaped ROIs were set on the bilateral frontal, parietal and occipital lobes and on the bilateral thalami and cerebellar hemispheres (Fig. 2). On the HP images, arbitrarily shaped ROIs were set on the bilateral medial and the lateral temporal lobes. The set of ROIs in the first SPECT study was transferred to the second SPECT study without changing the size, shape or position. The mean pixel count in each ROI was normalized to the mean pixel count of the global cerebral cortex.

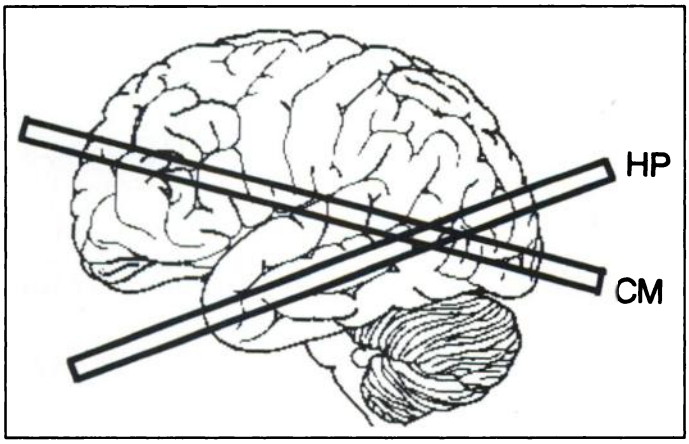

FIGURE 1. Reconstruction of hippocampal plane (HP) images. Transaxial slices were transformed into HP images, which were parallel to the longitudinal axis of the temporal lobes. The HP was inclined approximately 30° downwards from the cantho-meatal (CM) plane.

Statistical Analysis

The significance of differences was examined by Wilcoxon signed ranked test in 12 hemispheres. Differences were considered significant at $p < 0.05$.

RESULTS

Mean pixel count of the global cerebral cortex were 1088 ± 121 (mean ± s.d.) counts/pixel and 1261 ± 265 counts/pixel in ^{99m}Tc-HMPAO and ^{99m}Tc-ECD SPECT images, respectively. The results are summarized in Table 1. The relative distributions of ^{99m}Tc-HMPAO and ^{99m}Tc-ECD differed from each other in every region examined. In the frontal lobes, thalami, cerebellum and temporal lobes, ^{99m}Tc-HMPAO accumulated more than ^{99m}Tc-ECD did. By contrast, ^{99m}Tc-ECD accumulated more in the occipital and parietal lobes than did ^{99m}Tc-HMPAO. However, the differences between ^{99m}Tc-HMPAO and ^{99m}Tc-ECD distributions in the frontal and parietal lobes were small enough (2.6% and 1.8%) to be neglected in visual assessment of rCBF distribution. In the medial temporal lobes, the difference was most obvious among the seven regions examined. The mean relative accumulation levels of ^{99m}Tc-ECD and ^{99m}Tc-HMPAO in the medial temporal lobe were 83.1% ± 4.1% (mean ± s.d.) and 93.9% ± 2.4% of the mean cerebral cortical activity, respectively.

Figure 3 shows the HP images from an individual who showed considerable discrepancy between ^{99m}Tc-HMPAO and ^{99m}Tc-ECD accumulation in the medial temporal lobes. In this volunteer, it was equivocal which of the ^{99m}Tc-labeled tracers agreed with the relative CBF distribution in the medial temporal lobes measured by PET.

TABLE 1
Regional Distribution of Technetium-99m-HMPAO and Technetium-99m-ECD in Normal Brain

Region	Mean ROI size (Pixels)	Relative accumulation ^{99m}Tc-HMPAO (%)	Relative accumulation ^{99m}Tc-ECD (%)	p
Frontal lobe	84	102.2 (1.4)	99.6 (3.1)	0.021
Parietal lobe	75	99.5 (2.8)	101.3 (2.0)	0.027
Occipital lobe	102	103.6 (3.6)	106.8 (4.2)	0.001
Thalamus	30	110.2 (3.1)	101.4 (3.8)	<0.001
Cerebellum	112	108.3 (5.7)	99.6 (8.4)	<0.001
Lateral temporal lobe	79	98.3 (4.1)	93.3 (3.2)	0.002
Medial temporal lobe	51	93.9 (2.4)	83.1 (4.1)	<0.001

Data are expressed as the mean percent activity against the mean of the global cerebral cortex. Standard deviations are in parentheses.

DISCUSSION

In this study, we demonstrated that there is less accumulation of ^{99m}Tc-ECD than ^{99m}Tc-HMPAO in the normal medial temporal lobes. One participant in this investigation had an

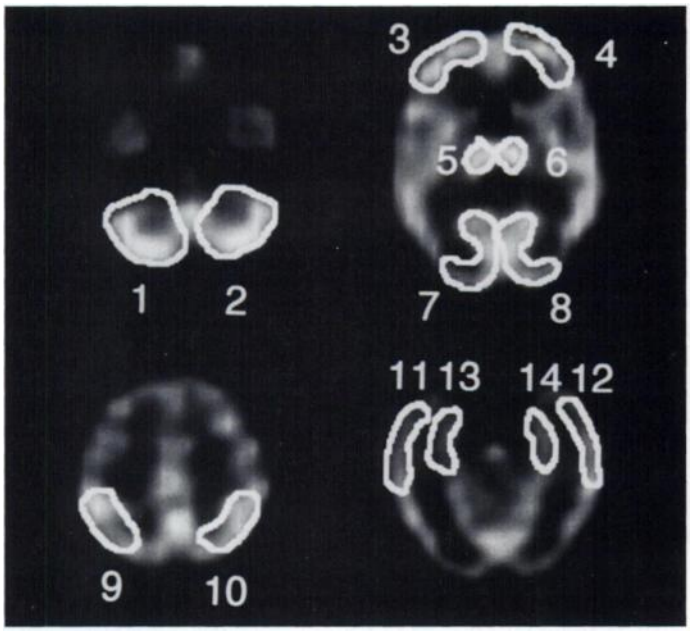

FIGURE 2. Arbitrarily shaped ROIs were set on the bilateral major parts of the brain. The medial and lateral sides of the temporal lobe were analyzed separately (bottom, right). 1 and 2 = right (R) and left (L) cerebellar hemispheres, 3 and 4 = R and L frontal lobes, 5 and 6 = R and L thalami, 7 and 8 = R and L occipital lobes, 9 and 10 = R and L parietal lobes, 11 and 12 = R and L lateral temporal lobes, 13 and 14 = R and L medial temporal lobes.

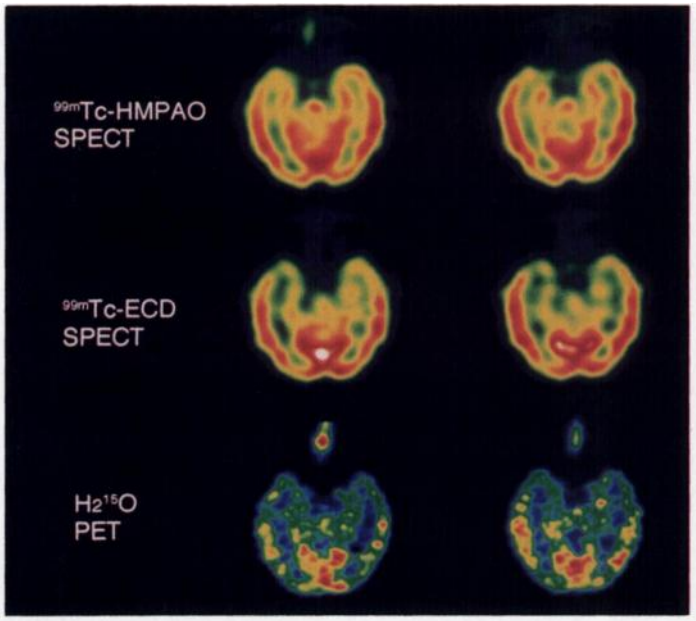

FIGURE 3. Comparison of hippocampal plane images among ^{99m}Tc-HMPAO SPECT, ^{99m}Tc-ECD SPECT and $H_2{}^{15}O$ PET. A 41-yr-old healthy man had two SPECT studies and a $H_2{}^{15}O$ PET study. There was considerable discrepancy in visualizing the medial temporal lobes between ^{99m}Tc-labeled tracers. The rCBF distribution measured by PET, $H_2{}^{15}O$ bolus injection and autoradiography was compared. Relative activity of ^{99m}Tc-HMPAO and ^{99m}Tc-ECD and the relative blood flow in the medial temporal lobe measured by SPECT and PET were 97%, 88% and 92% of the global cerebral cortex, respectively.

additional PET study for comparison of rCBF in the medial temporal lobes including the hippocampus, with accumulation of the two ^{99m}Tc-labeled tracers. However, since the results were ambiguous, it remains unknown which of the ^{99m}Tc-labeled tracers reflects true hippocampal rCBF. There are some explanations for this phenomenon. First, the accumulations of ^{99m}Tc-HMPAO and ^{99m}Tc-ECD are affected by glutathione and nonspecific esterase activity, respectively. The cortical distribution of these amino acids or enzymes is not uniform in the brain (*5*). Thus, structural or functional heterogeneity of the brain might cause this phenomenon. Second, it is also possible that spillover from high extracerebral ^{99m}Tc-HMPAO activity affected the medial temporal lobe that is adjacent to the internal carotid arteries and sphenoidal sinuses. Third, the contribution of regional metabolism to the accumulation of ^{99m}Tc-HMPAO and ^{99m}Tc-ECD might differ. The PET study of Takeda et al. (*6*) suggested that the ratio of rCBF in the hippocampus versus that in the superior frontal cortex was higher than the ratio of oxygen metabolism in the hippocampus versus that in the superior frontal cortex. The quantitative glucose metabolism measurement by Duara et al. (*7*) showed that the ratio of glucose metabolic rate in the hippocampus versus that in the cerebral gray matter was as low as 0.79. Our findings agreed with those results, assuming that the accumulation of ^{99m}Tc-ECD was more sensitive to the level of metabolism than was ^{99m}Tc-HMPAO.

These results will affect the diagnosis of temporal lobe pathology. The medial temporal lobe contains important structures, such as the hippocampus, amygdala and parahippocampal gyrus, that play key roles in the memory network (*8*). Recent studies (*9,10*) have shown that the hippocampus is one of the areas involved in the pathological changes associated with early Alzheimer's disease. Okazaki et al. (*11*) reported that HP images obtained using ^{99m}Tc-HMPAO and high-resolution SPECT could separate clearly the medial from the lateral temporal lobes, and observed hypoperfusion in the medial temporal lobe in possible Alzheimer's disease patients. Ohnishi et al. (*4*) indicated in their study using ^{99m}Tc-HMPAO that the degree of hypoperfusion in the medial temporal lobe was associated with the degree of cognitive impairment. Our results indicate that the hypoaccumulation of ^{99m}Tc-ECD in the medial temporal lobes should not be associated automatically with cognitive impairment in a patient suspected of having Alzheimer's disease.

Temporal lobe epilepsy (TLE) is known also as a functional disorder, the main pathology of which is located in the hippocampus (*12*). Neuroperfusion SPECT imaging is of considerable help in diagnosing the hemisphere responsible for epilepsy. In the interictal period, the epileptic focus usually appears as a low perfused area. Due to the nature of ^{99m}Tc-ECD, which accumulates less in the normal medial temporal lobes than does ^{99m}Tc-HMPAO, visual inspection of ^{99m}Tc-ECD neuroperfusion images in TLE patients might increase false-positive diagnoses and decrease specificity and accuracy.

CONCLUSION

Differential accumulations of ^{99m}Tc-ECD and ^{99m}Tc-HMPAO occur in the normal medial temporal lobes. The results suggest that ^{99m}Tc-HMPAO and ^{99m}Tc-ECD require specific and separate criteria for diagnosing temporal lobe pathologies, such as dementia and TLE. Further investigation is necessary to determine which ^{99m}Tc-labeled tracer is more sensitive or more specific for diagnosing temporal lobe pathology.

ACKNOWLEDGMENTS

We thank Mr. K. Fujino, of Osaka University Medical school hospital, and Mr. Y. Sekii, of Sumitomo Heavy Industry Co., for technical support in PET rCBF measurement. We also thank Miss M. Shimomura and Miss R. Manabe for administrative assistance. This work was supported in part by a research grant for cerebrovascular disease from the Ministry of Health and Welfare in Japan.

REFERENCES

1. Nakagawara J, Nakamura J, Takeda R, et al. Assessment of postischemic reperfusion and Diamox activation test in stroke using ^{99m}Tc-ECD SPECT. *J Cereb Blood Flow Metab* 1994;14:S49–S57.
2. Kimura K, Hashikawa K, Etani H, et al. A new apparatus for brain imaging: four-head rotating gamma camera single-photon emission computed tomograph. *J Nucl Med* 1990;31:603–609.
3. Kanno I, Iida H, Miura S, et al. A system for cerebral blood flow measurement using an $H_2{}^{15}O$ autoradiographic method and positron emission tomography. *J Cereb Blood Flow Metab* 1987;7:143–153.
4. Ohnishi T, Hoshi H, Nagamachi S, et al. High-resolution SPECT to assess hippocampal perfusion in neuropsychiatric diseases. *J Nucl Med* 1995;36:1163–1169.
5. Perry TL, Berry K, Hansen S, Diamond S, Mok C. Regional distribution of amino acids in human brain obtained at autopsy. *J Neurochem* 1971;18:513–519.
6. Takeda H, Nagata K, Hirata Y, et al. Age-related decline of cerebral oxygen metabolism in normal population detected with positron emission tomography. *Neurol Res* 1992;14:S128–S131.
7. Duara R, Margolin RA, Robertson-Tchabo EA, et al. Cerebral glucose utilization, as measured with positron emission tomography in 21 resting healthy men between the ages of 21 and 83 years. *Brain* 1983;106:761–775.
8. Zola-Morgan S, Squire LR. Neuroanatomy of memory. *Ann Rev Neurosci* 1993;16: 547–563.
9. Kazee AM, Eskin TA, Lapham LW, Gabriel KR, McDaniel KD, Hamill RW. Clinicopathologic correlates in Alzheimer disease: assessment of clinical and pathologic diagnostic criteria. *Alzheimer Dis Assoc Disord* 1993;7:152–164.
10. De Lacoste M, White CL. The role of cortical connectivity in Alzheimer's disease pathogenesis: a review and model system. *Neurobiol Aging* 1993;14:1–16.
11. Okazaki Y, Hashikawa K, Tanabe H, et al. Significance of hippocampal blood flow in the diagnosis of Alzheimer disease: survey by means of SPECT images longitudinally parallel to the hippocampus [Abstract]. *J Nucl Med* 1992;33(Suppl):940.
12. Hudson LP, Munoz DG, Miller L, McLachlan RS, Girvin JP, Blume WT. Amygdaloid sclerosis in temporal lobe epilepsy. *Ann Neurol* 1993;33:622–631.